Molecular Crystals and Liquid Crystals

Publication details, including instructions for authors and subscription information:
http://www.tandfonline.com/loi/gmcl20

Electrically Switchable Two-Dimensional Penrose Quasi-Crystal

Suraj P. Gorkhali [a] , Gregory P. Crawford [a] & Jun Qi [b]

[a] Division of Engineering, Brown University, Providence, RI, USA

[b] Wavefront Technology, Inc, Paramount, CA, USA

Version of record first published: 31 Aug 2006

To cite this article: Suraj P. Gorkhali, Gregory P. Crawford & Jun Qi (2005): Electrically Switchable Two-Dimensional Penrose Quasi-Crystal, Molecular Crystals and Liquid Crystals, 433:1, 297-308

To link to this article: http://dx.doi.org/10.1080/15421400590955730

Mol. Cryst. Liq. Cryst., Vol. 433, pp. 297–308, 2005

ISSN: 1542-1406 print/1563-5287 online
DOI: 10.1080/15421400590955730

Taylor & Francis
Taylor & Francis Group

Electrically Switchable Two-Dimensional Penrose Quasi-Crystal

Suraj P. Gorkhali
Gregory P. Crawford
Division of Engineering, Brown University, Providence, RI, USA

Jun Qi
Wavefront Technology, Inc, Paramount, CA, USA

We present the fabrication of a quasi-crystal liquid crystal polymer morphology using holographic polymer dispersed liquid crystal (H-PDLCs). By interfering five coherent, laser beams on a liquid crystal polymer mixture, a quasi-crystal morphology can be created on the mesoscale. We present scanning electron microscope (SEM) images mapped onto the calculated irradiance profiles confirming the quasi-crystal structure. Diffraction and electro-optic data are presented in the context of potential photonic applications.

Keywords: grating; H-PDLC; penrose; quasi-crystal

1. INTRODUCTION

The ability to utilize liquid crystals to create electrically switchable grating devices has resulted in a number of compelling application ideas in many industries including displays [1], telecommunications [2], and security [3]. One of the most studied liquid crystal switchable grating technology utilizes dispersions of liquid crystals and polymer which is based on a photo-assisted diffusion process [4]. These materials are known as holographic polymer dispersed liquid crystal (H-PDLCs). There are a number of review articles in the literature that describe their basic fabrication and operation [5–10], and a number of recent papers disclosing the material formulation used to create

We wish to acknowledge the National Science Foundation (EEC-0322878) for their financial support.

Address correspondence to Gregory P. Crawford, Division of Engineering, Brown University, Box D Providence, RI 02912, USA. E-mail: gregory_crawford@brown.edu

H-PDLC devices. One-dimensional gratings have been prepared for displays applications [11], telecommunications [12,13], strain gauges [14], beam steering [15], and lasing [16,17].

More recently, multidimensional H-PDLC gratings have been fabricated by Bowley [18]. Using a four beam exposure technique, Bowley and coworkers showed both reflection and diffraction versatility in a single film. These early studies were followed by the desire to construct well organized mesoscale lattices in H-PDLC materials. Several lattices have been reported in the literature including face-centered cubic [6,19], transverse square lattice [20], diamond like lattice [21] and other orthorhombic lattices [22,23]. In order to decouple the multi beams Qi and coworkers have demonstrated a temporal exposure technique to create distinct reflection bands [24]. These well defined Bravais lattice are being developed for photonic crystal applications because of their switching functionality and their flexible

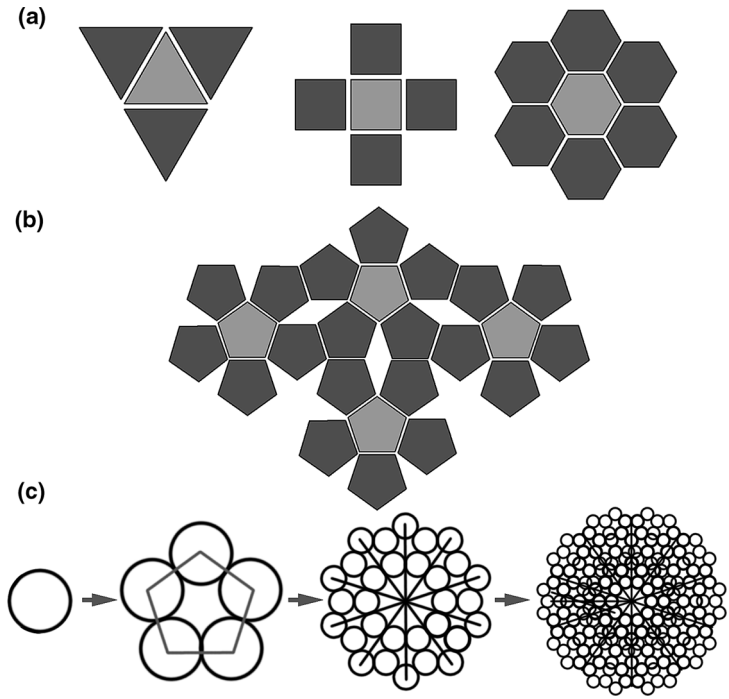

FIGURE 1 (a) Triangular, square and hexagonal tiling to fill up the entire 2D space (b) Five-fold pentagonal tiles packed together cannot fill the 2D space completely. (b) Five-fold overlapping packing of circles to create Penrose structure.

fabrication process enabling the creation of all Bravais lattice types in two and three dimensions [25].

In this contribution we extend our work on photonic lattice to those with quasi crystal symmetry in an attempt to understand, explore and design elegant optical devices. It has been demonstrated that two dimensional quasi-periodic lattice structures can be created in polymer resin using the holographic lithography method [26]. Here we present a five beam exposure technique to form a Penrose quasi crystal symmetry that can be turned on and off by the application of an electric field.

2. QUASI CRYSTAL DEFINITION

Geometrical constraint limits the lattice points in a crystal to only one, two, three, four and six-fold symmetry to fill up the entire space [27]. A two dimensional surface can completely covered with triangular, square, or hexagonal tiles representing three, four and six fold symmetry, as shown in Figure 1(a), without any left over spaces. However, when a pentagon is used in tiling (pentiling) a very different outcome is observed. Pentiling is defined as an arrangement of regular pentagons in the plane of the surface in which each pentagon makes edge-to-edge contact with two, three, four or five neighbors, thus sharing vertices in such a way that no gap can contain another entire pentagon. One example is shown in Figure 1(b). The quasi-lattice concept is a unique crystallographic concept in which the unit cell repeats along its symmetry axis and overlaps each other in a complex manner to fill up space. Five-fold overlapping quasi-periodic arrangement of the circles, representing unit cells, is shown in Figure 1(c). The arrangement is created by simply rotating a circle about an arbitrary point by $2\pi/5$ to create a larger five fold structure. This is repeated until the surface is filled with a Penrose pattern. This concept of the quasi-crystal was first introduced by Elser and Henley [28] following the realization that lattice structures with five-fold symmetry can fill up space in natural alloys [29]. Quasi-crystals exhibit fold symmetry but no overall absolute translational symmetry. Locally their environment demonstrates an overlapping translation and multi-fold symmetry. This local overlapping periodicity acts like a superimposed grating giving rise to multiple forbidden frequencies or photonic band gaps on the same plane.

3. QUASI CRYSTAL DESIGN IN H-PDLCS

We use N-beams with the same polar angle and equally distributed along azimuth plane to create a 2D N-fold quasi-periodic irradiance

pattern. The irradiance profile is generated from the interference of multiple coherent beams in a linear, isotropic medium and it can be generalized as the vector sum of electric fields [30]

$$I(\mathrm{r}) \propto R\left\{\sum_{l=1}^{N}\sum_{m=1}^{N}\mathrm{E}_l\mathrm{E}_m e^{i(\mathrm{K}_l-\mathrm{K}_m)\cdot\mathrm{r}}\right\} = R\left\{\sum_{l=1}^{N}\sum_{m=1}^{N}\mathrm{E}_l\mathrm{E}_m e^{i(\mathrm{G}_{lm})\cdot\mathrm{r}}\right\} \quad (1)$$

where $\boldsymbol{I}$ is the resulting intensity, $\mathbf{r}$ is the special position vector, N is the number of coherent beams, $\mathbf{K}_l$ is the wave vector and $\mathbf{G}_{lm}$ is the reciprocal lattice vector. In-plane and 3D views of the computer generated irradiance pattern for 5, 7 and 9-fold quasi-structure along with beam vectors and polarization are shown in Figure 2. The azimuth angle between the incident beams are 360°/5, 360°/7 and 360°/9 to create the 5, 7 and 9 fold quasi-crystal structure. The profile repeats

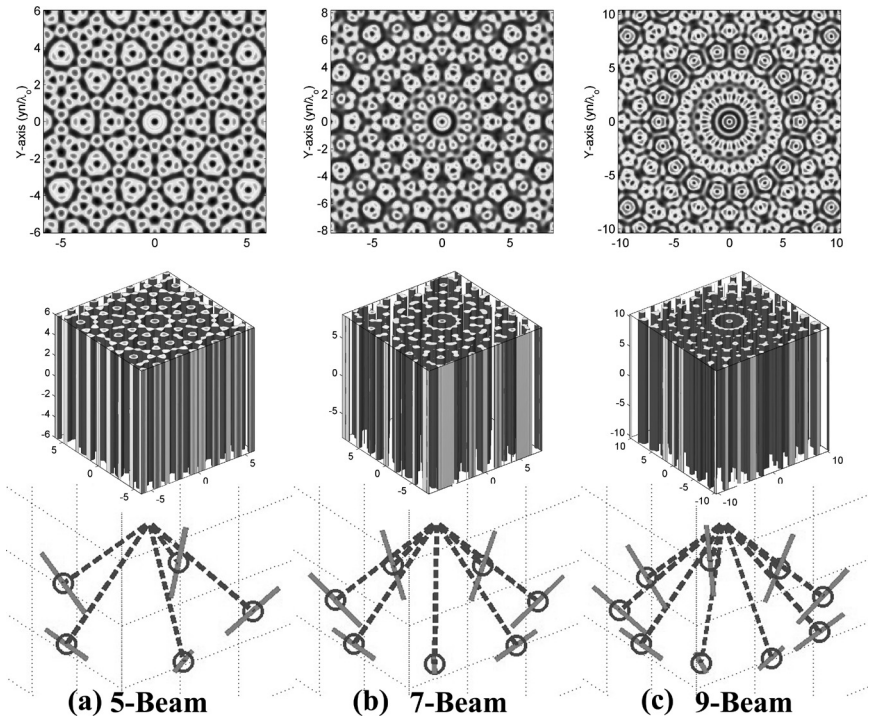

FIGURE 2 In-plane (top) and 3D (middle) view of irradiance pattern for 5, 7, and 9 fold symmetry quasi-crystal design. Beam vectors and polarization angles used to generate corresponding irradiance pattern (bottom).

in the third dimension creating a channel-like structure. We choose a five-fold Penrose quasi-periodic arrangement to further explore the quasi-crystal concept in H-PDLCs and present its design, fabrication, electro-optical properties.

4. FABRICATION METHOD

Five beams with the same polar angle, θ, of 28.9° and the azimuth angle, ϕ, of 72° to each other are interfered to create a 2D Penrose interference pattern. The computed irradiance pattern for the Penrose structure using these parameters is shown in Figure 2(a). The gray scale in the images in Figure 2 represents the resulting intensity; where white and black represent the destructive and constructive interference regions respectively. A schematic diagram of the optical apparatus used for the Penrose exposure is illustrated in Figure 3. Five equal intensity, p-polarized, mutually coherent laser beams are produced by splitting a single 532 nm laser beam. The samples are prepared using a standard H-PDLC fabrication process. The photo reactive mixture used was a homogenous mixture of 43 wt.% aliphatic urethane resin oligomers (Ebecryl 8301 and Ebecryl 4866 oligomers from *UCB Chemicals*), 35 wt.% nematic liquid crystal BL038 from *EM Industries*, 12 wt.% Rose Bengal-based photoinitiator solution, and 10 wt.% surfactant S-271 (*Chem Service*). A similar version of this

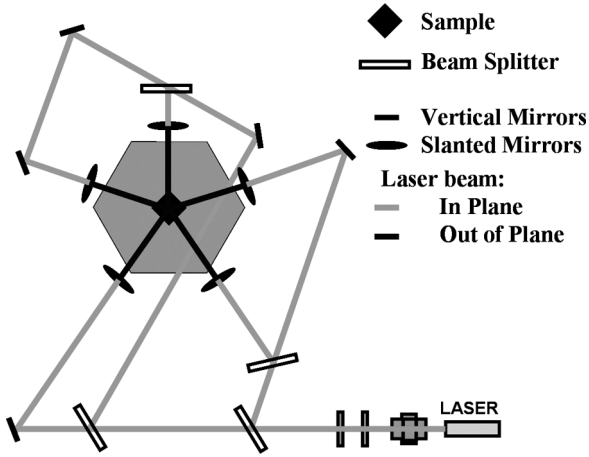

FIGURE 3 Schematic diagram of the optic table setup used to fabricate Penrose quasi-crystal with five equal intensity p-polarized laser beams using H-PDLC method.

mixture has been reported earlier in the literature [4]. The photosensitive visible H-PDLC mixture is sandwiched between two conducting glass plates coated with Indium Tin Oxide (ITO). The 10 μm fiber spacers between the plates precisely maintain spacing between the glass plates to control the sample thickness. The sample is then exposed to the interference pattern as described earlier. Photo polymerization occurs in the high intensity regions which in turn initiates photo-induced diffusion of the LC to the dark regions. This phase separation of LC and polymer continues until the monomer is completely polymerized. The final product consists of the liquid crystal and polymer morphology mimicking the irradiance pattern where the LC is spatially positioned in the low intensity region and the polymer position in the high intensity region, permanently capturing the computed two-dimensional Penrose quasi-periodic structure in H-PDLC material.

The wave vectors of the five beams that interfere to produce the Penrose interference pattern are $\mathbf{K_1} = [1, 0, 1.8]$, $\mathbf{K_2} = [\cos(\alpha), \sin(\alpha), 1.8]$, $\mathbf{K_3} = [\cos(\alpha), -\sin(\alpha), 1.8]$, $\mathbf{K_4} = [-\cos(\alpha/2), \sin(\alpha/2), 1.8]$ and $\mathbf{K_5} = [-\cos(\alpha/2), -\sin(\alpha/2), 1.8]$, where α is $2\pi/5$. Figure 4 shows the wave vectors of the beams and corresponding reciprocal vector geometry of the interference pattern. Five solid arrows drawn from the center of the pentagon represents the wave vectors of the five beams. The reciprocal lattice vectors are determined by the difference of the wave vectors. i.e. $\mathbf{K_1} - \mathbf{K_2} = \mathbf{G_{12}}$. Five of the reciprocal lattice

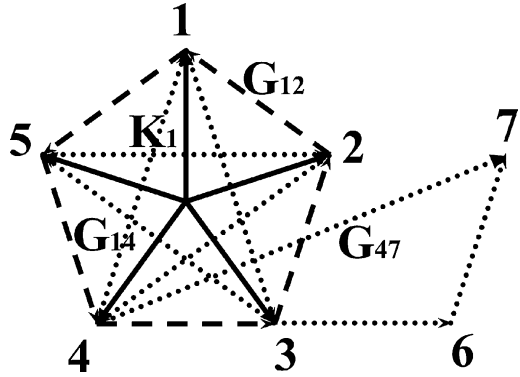

FIGURE 4 Reciprocal vector geometry for a Penrose pattern. The black arrows are the wave vectors of five beams. The dashed and dotted line vectors inside the pentagon show the first and second order reciprocal lattice vectors, respectively. The vector G_{47} is the third order reciprocal lattice vector which is a combination of three first order reciprocal lattice vectors.

vectors $\mathbf{G_{12}}$, $\mathbf{G_{23}}$, $\mathbf{G_{34}}$, $\mathbf{G_{45}}$, and $\mathbf{G_{51}}$, represented by the dashed line vectors at the edges of the pentagon, form the basis of the reciprocal space. The dotted line vectors inside the pentagon show the second order reciprocal lattice vectors which is the sum of two first order vectors. The vector $\mathbf{G_{47}}$ is the third order reciprocal lattice vector which is a combination of three first order lattice vectors. The reciprocal lattice vector determines the resulting structure formed in real space. The pitch in the sample or the repeating lattice structure is calculated using Bragg's law. Using 532 nm green laser construction beams the calculated pitch corresponding to reciprocal lattice vectors $\mathbf{G_{12}}$, $\mathbf{G_{14}}$ and $\mathbf{G_{47}}$ are $\Lambda_1 = 1.15\,\mu\text{m}$, $\Lambda_2 = 1.87\,\mu\text{m}$, $\Lambda_3 = 0.79\,\mu\text{m}$ respectively. The diffraction pattern produced by the same 532 nm incident light on the Penrose sample can be calculated. The ten first order diffraction spots, as a result of left and right set of reciprocal lattice vector, will have the cone angle of 16.5° and are separated by $\phi = 36^\circ$. Similarly ten spots at cone angle 27.4°, 34.7° and 67.3° are produced by other higher order combinations.

5. DISCUSSION AND RESULTS

5.1. Diffraction Pattern

The visible diffraction pattern observed when probing the sample with a green laser ($\lambda = 532\,\text{nm}$), clearly reveals the presence of Penrose quasi-periodicity within the sample as shown in Figure 5(a). In Table 1, we compare the angle of the measured diffraction spots to the calculated ones in the previous section. The transmission diffraction pattern produced by a normally incident laser beam has a perfect 10-fold symmetry. Diffraction spots disappear upon the application of an applied voltage indicating that the index of refraction of the polymer is nearly matched to the ordinary index of refraction of the liquid crystal [31] removing the in-plane quasi-periodic refractive index modulation. Figure 5(b) shows the diffraction pattern from the sample using a broad band focused white light.

5.2. Scanning Electron Microscopy (SEM) Study

The scanning electron microscopy (SEM) was used to investigate the polymer morphology. The samples were prepared in a similar way as those reported in the literature [32]. Figure 6(a) shows the SEM images of the formed quasi-crystal structure. The bubble contours are the polymer enclosure that are raised up by the expansion of the LC droplet trapped underneath during the heating process.

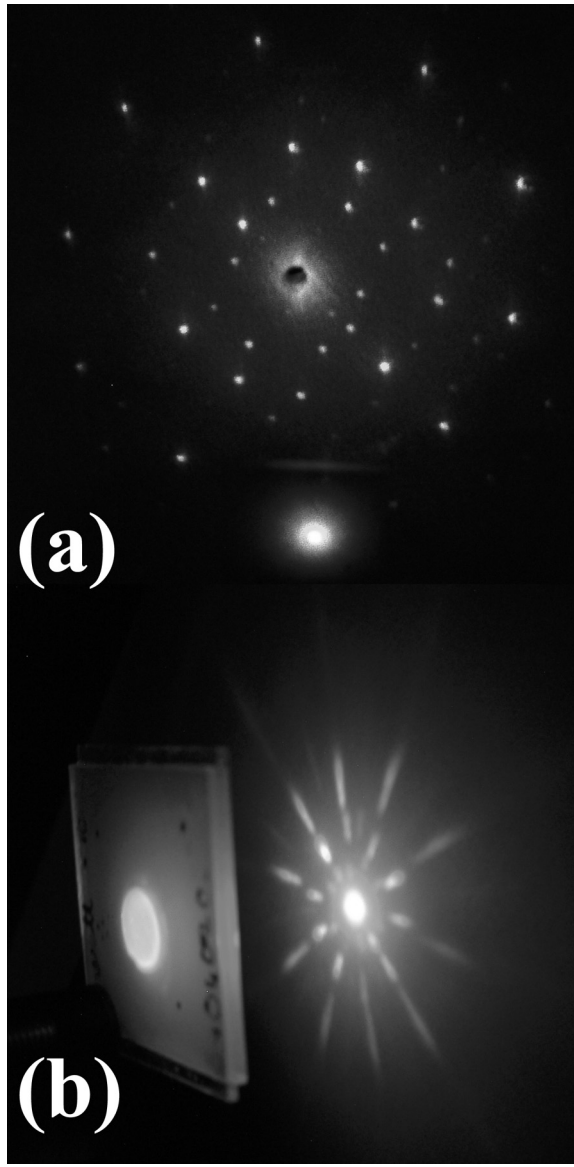

FIGURE 5 (a) Diffraction pattern using a Green wavelength laser ($\lambda = 532\,\text{nm}$). Zero order diffraction spot is dumped into the beam stop to make the higher order spots easily visible in the picture. (b) Full color diffraction pattern from a Penrose H-PDLC sample using a broad band focused white light.

TABLE 1 Calculated and the Measured Diffraction Cone Angle Produced by 532 nm Green Laser Incident on the Penrose Sample and the Corresponding Pitch Length

Order	1st	2nd	3rd	4th
Pitch	1.87 μm	1.15 μm	0.94 μm	0.75 μm
Calculated	16.5°	27.4°	34.7°	45.3°
Measured	$18^\circ \pm 2^\circ$	$28^\circ \pm 2^\circ$	$35^\circ \pm 2^\circ$	$47^\circ \pm 2^\circ$

Figure 6(b) show the computer generated unit cell irradiance pattern compared with the SEM image. The white spots correspond to the destructive interference regions in which the LC droplets are formed. The computed LC spots, represented by dark outline on the right half of Figure 6(c), are superimposed on the SEM image to show the close comparison between the calculated intensity profile and the SEM images. Nearly all calculated LC droplet positions overlapped the corresponding LC droplet in the SEM. The shape and the orientation of the droplet also correspond well to the calculated intensity profile. The theoretical five-fold overlapping quasi-periodic arrangement of the circles from Figure 1(b) is also superimposed on top of the SEM represented in Figure 6(c). These results confirm the existence of five-fold quasi-periodic distribution of LC droplets within the polymer binder and demonstrate the accuracy and consistency of H-PDLC method to fabricate quasi structures.

5.3. Electro-Optical Characteristics

Figure 7 shows diffraction efficiency for the first order diffraction spot, which diminishes upon the application of an applied voltage. The switching time for the first order diffraction spot was measured to be ~1 ms. The diffraction efficiency of a single first order diffraction spot is approximately 1.5%, and we estimate that the refractive index modulation is $\sim 3 \times 10^{-3}$ using a coupled wave theory [33]. The optical efficiency and switching time depends on various factors like liquid crystal and polymer formation, droplet size, shape, and also the basic properties of LC used (elastic constant, birefringence, dielectric anisotropy and viscosity). Compared to visible reflecting H-PDLCs, the response time is slightly longer due to the micron-sized LC droplets. The enhancement of the phase separation conditions is essential to improve the optical properties of the quasi-crystals, which can be achieved by varying the exposure intensity. The utilization

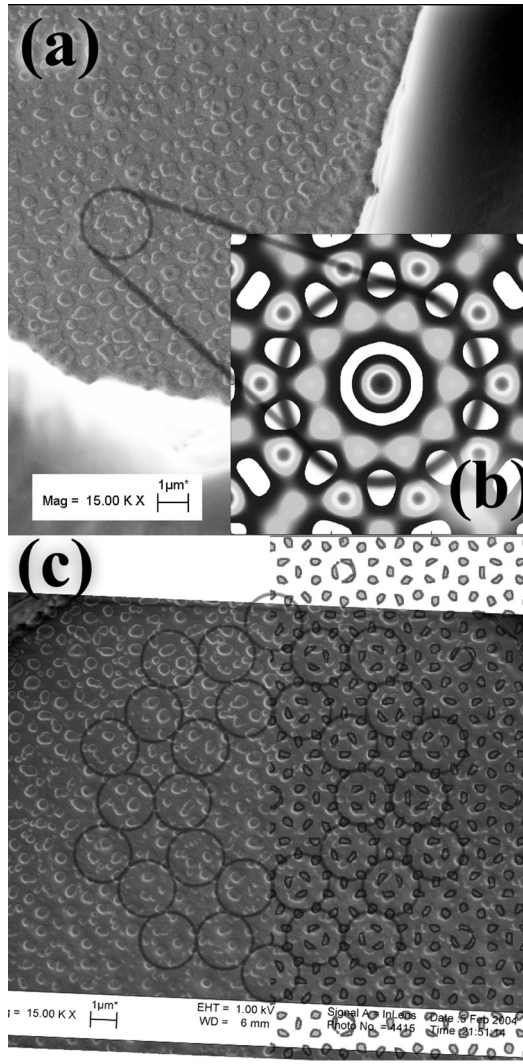

FIGURE 6 (a) SEM image of the quasi-crystal generated by H-PDLC method shows the LC bubble bounded within polymer structure. (b) Computer generated irradiance pattern compared with SEM image showing the basic five fold structure. Gray scale gradient represents the intensity, and white and black represent the destructive and constructive interference regions respectively. (c) Destructive interference regions from the computer generated Penrose model, represented by dark outline on the right half of the image, is superimposed on top of the SEM image showing the perfectly captured liquid crystal droplets in Penrose quasi structure. The theoretical five-fold overlapping quasi-periodic arrangement of the circles from Figure 1(b) is also superimposed on top.

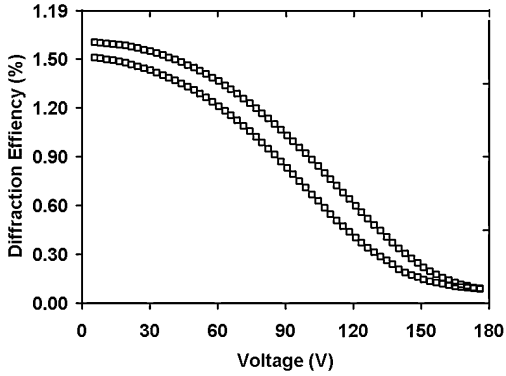

FIGURE 7 Diffraction efficiency as a function of applied voltage.

of LCs with superior birefringence can also increase the index modulation, therefore the diffraction efficiency. We are currently in the process of optimizing this configuration for optical application.

6. CONCLUSION

We have successfully fabricated electrically switchable two-dimensional Penrose quasi-crystal.Transmission spectra, diffraction patterns and the SEM images were all consistent with the theoretical intensity model and anticipated optical results regarding the structure of a Penrose quasi-crystal structure. Further studies include 7 and 9 fold symmetry, and further optimization of the Penrose structure for evolution as photonic switches.

REFERENCES

[1] Tanaka, K., Kato, K., & Date, M. (1999). *Jpn. J. Appl. Phys.*, *38*, L277.
[2] De Bougrenet De La Tocnaye, J. L. (2004). *Liquid Crystals*, *31*(2), 241.
[3] Renesse, R. L. (1997). *Optical Document Security*, Artech House Publishers: Boston.
[4] Bowley, C. C. & Crawford, G. P. (2000). *Appl. Phys. Lett.*, *76*, 2235.
[5] Crawford, G. P. (2003). *Optics and Photonics News*, *4*, 54.
[6] Escuti, M. J., Qi, J., & Crawford, G. P. (2003). *Opt. Lett.*, *28*, 522.
[7] Pogue, R. T., Sutherland, R. L., Schmitt, M. G., Natarajan, L. V., Siwecki, S. A., Tondiglia, V. P., & Bunning, T. J. (2000). *Applied Spectroscopy*, *54*, 12A–28A.
[8] Bunning, T. J., Natarajan, L. V., Tondiglia, V. P., & Sutherland, R. L. (2000). *Annu. Rev. Mater. Sci.*, *30*, 83–115.
[9] Sutherland, R. L., Tondiglia, V. P., Natarajan, L. V., Bunning, T. J., & Adams, W. W. (1994). *Appl. Phys. Lett.*, *64*, 1074.
[10] Tondiglia, V. P., Natarajan, L. V., Sutherland, R. L., Tomlin, D., & Bunning, T. J. (2002). *Adv. Mater.*, *14*, 187.

[11] Tanaka, K., Kato, K., Tsuru, S., & Sakai, S. (1994). *J. Soc. Inf. Disp.*, *2*, 37.
[12] Domash, L. H., Crawford, G. P., Ashmead, A. C., Smith, R. T., Popovich, M. M., & Storey, J. (2000). *Proceedings from SPIE*, **4107**, 46.
[13] Yeralan, S., Gunther, J., Ritums, D., Cid, R., & Popovich M. (2002). *Optical Engineering*, *41*(8), 1774.
[14] Cairns, D. R., Bowley, C. C., Danworaphong, S., Fontecchio, A. K., Crawford, G. P., Li, L., & Faris, S. M. (2000). *Appl. Phys. Lett.*, *77*, 2677.
[15] Domash, L. H., Crawford, G. P., Ashmead, A. C., Smith, R. T., Popovich, M. M., & Storey, J. (2000). *Proc. SPIE* **4107**, 46.
[16] He, G. S., Lin, T., Hsiao, V. K. S., Cartwright, A. N., Prasad, P. N., Natarajan, L. V., Tondiglia, V. P., Jakubiak, R., Vaia, R. A., & Bunning, T. J. (2003). *Appl. Phys. Lett.*, *83*, 2733.
[17] Lucchetta, D. E., Criante, L., Francescangeli, O., & Simoni, F. (2004). *Appl. Phys. Lett.*, *84*, 837.
[18] Bowley, C. C., Fontecchio, A. K., Crawford, G. P., Lin, J., Li, L., & Faris, S. (2000). *Appl. Phys. Lett.*, *76*, 523.
[19] Campbell, M., Sharp, D. N., Harrison, M. T., Denning, R. G., & Tuberfield, A. J. (2000). *Nature*, *404*, 53.
[20] Escuti, M. J., Qi, J., & Crawford, G. P. (2003). *Appl. Phys. Lett.*, *83*, 1331.
[21] Escuti, M. J. & Crawford, G. P. *Mol. Crystl Liq. Cryst.*, (accepted for publication).
[22] Sutherland, R. L., Tondiglia, V. P., Natarajan, L. V., & Chandra, S. (2002). *Opt. Express*, *10*, 1074.
[23] Tondiglia, V. P., Natarajan, L. V., Sutherland, R. L., Tomlin D., & Bunning, T. J. (2002). *Adv. Mater.*, *14*, 187.
[24] Qi, J., Sousa, M. E., Fontecchio, A. K., & Crawford, G. P. (2003). *Appl. Phys. Lett.*, *82*, 1652.
[25] Cai, L. Z., Yang, X. L., & Yang, Y. R. (2002). *Opt. Lett.*, *27*, 900.
[26] Wang, E., Ng, C. Y., Tam, W. Y., Chan, C. T., & Sheng, P. (2003). *Adv. Mater.*, *15*(18), 1526.
[27] Rohrer, G. S. (2001). *Structure and Bonding in Crystalline Materials*, Cambridge University Press: New York, Chapter 3, 88.
[28] Elser, V. & Henley, C. L. (1985). *Physical Rev. Lett.*, *55*, 1883.
[29] Shechtman, D., Blech, I., Gratias, D., & Cahn, J. W. (1984). *Physical Rev. Lett.*, *53*, 1951.
[30] Born, M. & Wolf, E. (1999). *Principles of Optics*, Cambridge University Press: London.
[31] Doane, J. W., Vaz, N. A., Wu, B. G., & Zumer, S. (1986). *Appl. Phys. Lett.*, *48*, 269–271.
[32] De Sarkar, M., Qi, J., & Crawford, G. P. (2002). *Polymer*, *43*, 7335–7344.
[33] Kogelnik, H. (1969). *Bell Sys. Tech. J.*, *48*, 2909.